International Journal for Parasitology: Drugs and Drug Resistance 7 (2017) 110–119

Contents lists available at ScienceDirect

International Journal for Parasitology: Drugs and Drug Resistance

journal homepage: www.elsevier.com/locate/ijpddr

Quantitative characterization of hemozoin in *Plasmodium berghei* and *vivax*

John M. Pisciotta [a], Peter F. Scholl [b], Joel L. Shuman [c], Vladimir Shualev [c], David J. Sullivan [a, *]

[a] Department of Molecular Microbiology and Immunology, Johns Hopkins University, Bloomberg School of Public Health, 615 N. Wolfe St., Baltimore, MD 21205-2179, USA
[b] Department of Environmental Health Sciences, Bloomberg School of Public Health, Johns Hopkins University, Baltimore, MD 21205-2103, USA
[c] Virginia Bioinformatics Institute, Virginia Polytechnic Institute and State University, Blacksburg, VA 24061, USA

ARTICLE INFO

Article history:
Received 29 August 2016
Received in revised form
1 February 2017
Accepted 3 February 2017
Available online 8 February 2017

Keywords:
Hemozoin
Chloroquine resistance
Plasmodium berghei
Plasmodium vivax

ABSTRACT

The incidence and global distribution of chloroquine resistant (CR) *Plasmodium vivax* infection has increased since emerging in 1989. The mechanism of resistance in CR *P. vivax* has not been defined. The resistance likely relates to the formation and disposition of hemozoin as chloroquine's primary mechanism of action involves disruption of hemozoin formation. CR *P. berghei* strains, like CR *P. vivax* strains, are confined to reticulocyte host cells and reportedly they do not accumulate appreciable intraerythrocytic hemozoin. Reports comparing hemozoin production between *P. vivax* strains and CR to chloroquine sensitive (CS) *P. berghei* are absent. Here we compare *in vivo* patterns of hemozoin formation and distribution in blood, spleen and liver tissue of male Swiss mice infected with CS or CR *P. berghei* not treated with chloroquine and CR *P. berghei* also treated with chloroquine. Light microscopy, laser desorption mass spectrometry and a colorimetric hemozoin assay detect trace hemozoin in the blood of CR *P. berghei* infected mice but significant hemozoin accumulation in liver and spleen tissue. Field emission in lens scanning electron microscopy reveals CR *P. berghei* hemozoin crystals are morphologically smaller but similar to those formed by CS parasites. CR *P. berghei* produces approximately five-fold less total hemozoin than CS strain. Lipid analysis of CS and CR *P. berghei* sucrose gradient purified bloodstage hemozoin indicates a similar lipid environment around the isolated hemozoin, predominately monopalmitic glycerol and monostearic glycerol. In contrast to CR and CS *P. berghei*, colorimetric hemozoin analysis of *P. vivax* strains indicates similar amounts of hemozoin are produced despite differing chloroquine sensitivities. These results suggest CR *P. berghei* forms significant hemozoin which accumulates in liver and spleen tissues and that the *P. vivax* chloroquine resistance mechanism differs from *P. berghei*.

1. Introduction

Intraerythrocytic *Plasmodium* parasites ingest and catabolize host erythrocyte hemoglobin in a digestive vacuole that arises from invagination of the parasitophorous vacuolar membrane and the underlying parasite membrane (Yayon et al., 1984). Hemoglobin comprises an estimated 95% of the total protein content of the mature erythrocyte. Hemoglobin catabolism releases copious monomeric iron protoporphyrin IX, or heme, which oxidatively damages membranes and inhibits parasite catabolic enzymes (Orjih et al., 1994). *Plasmodium* parasites avert heme-mediated damage by sequestering heme into a relatively inert, brown, birefringent biocrystal called hemozoin. Chloroquine, a weak base, accumulates in the acidic digestive vacuole of drug sensitive parasites where it complexes free heme to cap and inhibit hemozoin elongation along the growing crystal face (Sullivan et al., 1996).

In chloroquine resistant (CR) *P. falciparum* a point mutation of the Pfcrt gene is associated with clinical treatment failure (Fidock et al., 2000). This mutation imparts a drug metabolite transporter mediated form of drug resistance that is verapamil-reversible

* Corresponding author. 615 North Wolfe Street, Suite E5628, Baltimore, MD 21205, USA.
E-mail address: dsulliv7@jhmi.edu (D.J. Sullivan).

http://dx.doi.org/10.1016/j.ijpddr.2017.02.001

(Howard et al., 2002). The Pfmdr1 gene codes for another transporter also associated with chloroquine resistance in *P. falciparum* (Foote and Kemp, 1989; Das et al., 2013). The mechanism of *P. vivax* chloroquine resistance is not understood. Experimental testing is hampered because *P. vivax* is difficult to culture *in vitro*. *P. vivax* chloroquine resistance arose decades after it was noted in *P. falciparum.* The molecular basis of resistance clearly differs as Pvcrt gene sequence analysis indicates no changes between resistant and sensitive *P. vivax* (Wellems and Plowe, 2001). Mutations of Pvmdr1 have not been found to impart chloroquine resistance in *P. vivax* amid conflicting clinical studies (Goncalves et al., 2014). One study found *P. vivax* chloroquine resistance was associated with enhanced expression of pvcrt-o and pvmdr-1 (Melo et al., 2014). However, a different human study found increases in pvmdr copy number were associated with resistance to mefloquine yet actually enhanced susceptibility to chloroquine (Vargas-Rodriguez Rdel et al., 2012). Transcriptional upregulation of wild type pvcg10 (pvcrt-o) transfected into CS *P. falciparum* facilitates reduced chloroquine susceptibility, if not full resistance, but no direct role for transporters in CR *P. vivax* parasites has been established (Sá et al., 2005).

Plasmodium berghei infects rodents and is considered a useful model for studying *P. vivax* infection and alternative forms of chloroquine resistance (Espinosa et al., 2013). This is because CR *P. berghei,* like *P. vivax,* infects only reticulocyte host cells (Ocampo et al., 2002). CR *P. berghei* also does not secrete chloroquine more rapidly than the CS strain (Wang et al., 1998). Treatment with the P-glycoprotein transporter inhibitor rifampicin or verapamil does not restore susceptibility in CR strains (Peters et al., 1990; Platel et al., 1998). Consistent with the lack of chloroquine resistance transporter (CRT) based mutations, these facts indicate *P. berghei* and *P. vivax* chloroquine resistance differs from the transporter mediated resistance seen in *P. falciparum*.

CR *P. berghei* strains have for decades been reported to form little or no hemozoin pigment (Peters, 1964). Lin et al. recently created CR *P. berghei* strains that form little to no hemozoin by knocking out genes in the CS wild type that are associated with hemoglobin catabolism (Lin et al., 2015). The CS wild type could infect reticulocytes and mature RBCs alike and form abundant hemozoin, but the CR knockouts could develop only in reticulocytes. Choroquine treatment of CS *P. berghei* reduces hemozoin formation by an order of magnitude and causes accumulation of deadly free heme; however, in CR *P. berghei* chloroquine treatment causes no detectable buildup of free heme (Fitch and Chou, 1997). Reduced glutathione (GSH), naturally elevated in reticulocytes, can degrade heme and might play a role in chloroquine resistance in *P. berghei* (Ginsburg et al., 1998). However, genetic upregulation of GSH does not impart chloroquine resistance to CS strain *P. berghei* (Vega-Rodriguez et al., 2015). Alternatively, membrane-bound heme and hemozoin may be ejected from reticulocytes using the native host reticulocyte process of exocytosis (Slomianny, 1990; Slomianny and Prensier, 1990). Hemozoin, if produced, would be expected to present in the liver and spleen tissue of mice infected with CR *P. berghei*. A shift to a circulating ring predominance in CR *P. berghei* with sequestration of trophozoites and schizonts in tissue (Jacobs and Warren, 1967; Schneider, 1968), also does not explain resistance to chloroquine as the sequestered parasites would have similar drug exposures. This study investigates *P. berghei* chloroquine resistance by investigating patterns of hemozoin formation and tissue distribution by multiple methods in CS and CR *P. berghei* parasites and their murine hosts. We also compared hemozoin formation in CR versus CS *P. vivax* isolates.

2. Materials and methods

2.1. P. berghei parasite strains and infection of host mice

Male Swiss mice (CF-1) weighing approximately 25 g were purchased from Sasco, Inc. (Omaha, Neb.). They were given Purina Laboratory Chow and water ad libitum, and their care was provided in accordance with Saint Louis University guidelines. At St. Louis University blood from NYU-2 strain CR *P. berghei* infected mice isolated in 1974 and kept under chloroquine pressure as well as the chloroquine sensitive parent were utilized (Fitch et al., 1974). The CR line had been passaged every 2 weeks for two years under chloroquine pressure applied by intraperitoneal injection of 1 mg of chloroquine daily on Monday through Friday of each week. Frozen stocks of CR *P. berghei* were inoculated into 6 mice with chloroquine treatment at 1 mg per mouse intraperitonealy dosed to revive the frozen isolate. After 14 days with parasitemia about 10% the infected blood was passaged to 12 mice with continued chloroquine treatment 5 days of the week. After another 14 days the combined blood was inoculated into two groups with one on continued chloroquine and another off chloroquine. The frozen CS line of NYU-2 *P. berghei* was inoculated to a control set of donor mice not treated with chloroquine and on day 9 post infection of the CR and CRCT, a new CS NYU-2 *P. berghei* was begun such that on the same day the CS mice would be exsanguinated on day 5 of infection and day 15 for the CR and CRCT groups. Each passage used 100 μl of a 1:25 dilution of 25–50% parasitemia or 10 to 20 million infected parasites per passage given by the intraperitoneal route. 16 young male Swiss mice of 25 g each were divided into 4 groups of 4 mice per group. Mice of the chloroquine treated CRCT group were treated with 40 mg/kg of chloroquine base per day. Mice of the uninfected negative control group received no drug. Mice of the positive control group infected with CS *P. berghei* (NYU-2 strain) and the CR *P. berghei* also recieved no drug. Before death and following a 5 day time post infection period for CS infected mice and a 15 day time post infection period for the CR and CR/CT groups, due to their lower parasitemia, mice were anesthetized and sacrificed by exsanguination. Hematocrit levels were measured and two thin blood smears were prepared for each mouse. One smear was methanol fixed and Geimsa stained to permit quantitation of total parasitemia per 1000 RBCs. The other was fixed with methanol only. Livers and spleens were recovered, weighed before processing in formalin for histology or frozen at −80 °C.

2.2. Tissue processing and hemozoin analysis

The mice were infected on two separate occasions. After the first experiment, the liver and spleen were divided and half placed into neutral formalin and half frozen for hemozoin quantification and electron microscopy. In the second biologic experiment 80% of liver and spleen from each mouse went for quantification of hemozoin. Mouse livers and spleens were divided and preserved in 10% neutral formalin. Formalin preserved liver and spleen samples were paraffin embedded and thin sectioned. Histological slides were hematoxylin and eosin (H+E) stained and examined via brightfield and polarizing light microscopy. Individual microscopic field overlaps at 400x and 1,000x were photographed under brightfield and polarized light to document brown, birefringent hemozoin crystals in tissue and blood smears. The cryogenically stored blood, plasma, spleen and liver samples were thawed and processed to purify, detect and quantify hemozoin. Briefly 400–500 μl of blood from each mouse were hypotonically lysed in 4.5 ml of DI H_2O. Individual mouse livers or spleens were homogenized in 5 mL of DI H_2O by pulsed sonication (Branson sonifier). Lysed blood and tissue were centrifuged at 14,000 times gravity for 15 min to pellet

hemozoin. The supernatant fraction was removed and the pellets resuspended in 1 ml 2% SDS, 100 mM sodium bicarbonate. This was spun down as above and the pellets washed in 2% SDS and centrifuged. Washed pellets were resuspended and incubated overnight at 60°C in 1 mg/ml proteinase K buffer. Following incubation, samples were washed in DI H_2O. Purified hemozoin pellets were then decrystallized in 1 ml 2% SDS 20 mM NaOH for 1 h and spectrophotometrically quantitated by measuring absorbance either in a Beckman DU-640 cuvette with a 1 cm pathlength with a molar extinction coefficient at 400 nm of 1×10^5 or in a Perkin Elmer HTS 7000 96 well plate reader in 200 μl with molar extinction coefficient of 5.7×10^4 with a 405 nm filter for the 200 μl volume.

2.3. Ultrastructure and LDMS examination of purified hemozoin

Purified hemozoin crystals from blood of CS *P. berghei* and from liver and spleens mixed together from separate infections of CS, CR, and CRCT *P. berghei* were examined via Field Emission Inlens Scanning Electron Microscopy (FEISEM). For this purified hemozoin pellets were resuspended in 10 μl DI H_2O, deposited onto FEISEM chips and dried in a vacuum chamber. Crystals were sputter coated with gold palladium and examined under the FEISEM (Leo 1530). Scanning electron micrographs of putative hemozoin crystals were taken.

Blood, plasma and homogenized liver and spleen samples were examined for the specific presence of hemozoin by direct ultraviolet laser desorption time-of-flight mass spectrometry laser desorption mass spectrometry (LDMS). Samples were thawed and blood was diluted 1:5 and 1:10 in DI H_2O. Homogenized tissue samples were further diluted as needed based upon colorimetric hemozoin quantitation to avoid detector plate saturation. 0.5 μl of the diluted samples were spotted in triplicate to individual wells on 192 well Applied Biosystems MALDI plate. Positive ion mass spectra in from 400 to 800 were obtained (*m/z*) using an Applied Biosystems Voyager DE-STR instrument located at the AB mass spectrometry facility in the Johns Hopkins University School of Medicine. Five laser shot sets each comprised of 20 individual laser shots randomly rastered across the spot's surface were conducted and each of the five sets scored as being positive or negative for the presence of hemozoin as indicated by the occurrence of the characteristic hemozoin heme mass spectrum. The mean base peak millivolt amplitude (mV) of the major fragmentation ion (*m/z* 497) for each shot set was recorded as a semi-quantitative indication of hemozoin concentration. Adjusted mV intensities were calculated based upon the initial dilution factor and amount of sample processed.

2.4. Subcellular fractionation and electrospray ionization mass spectrometery (ESI-MS) analysis of P. berghei hemozoin associated lipids

P. berghei parasites were isolated by saponin lysis of infected mouse erythrocytes. Hemozoin and associated material was isolated by ultracentrifugation through 1.7 M sucrose cushions as described previously (Sullivan et al., 1996). Lipids were extracted by chloroform methanol and processed as lithium adducts for ESI-MS according to Ham (Ham et al., 2004). At least two different biologic isolations on different dates for each of the parasite fractionations was analyzed by ESI-MS. Samples were infused and analyzed at flow rate of 20 μl per minute using a Thermo-Finnigan, TSQ quantum triple stage quadrapole ESI-MS/MS.

2.5. P. vivax monkey adapted strains and infection of primate hosts

Saimiri monkeys were infected with either the CS Salvador I strain *P. vivax* or the CR *P. vivax* Indonesian strain XIX at the Centers of Disease Control (Atlanta, GA). One additional *Aotus* monkey was infected with the CR *P. vivax* Indonesian strain XIX. Monkeys were housed with normal food and water and no drug treatment for a period of a 5–7 weeks. Periodic blood samples were taken and parasitemia determined by optical microscopy of 5 μl thick smears. Hemoglobin levels at time of exsanguination were estimated by OD 405 nm measurements of 2 and 4 μl of packed RBCs suspended in 100 μl of DI H_2O. Two blood samples from each monkey, approximately one ml each, were spun for 3 min at 3000x g and the plasma separated from pelleted packed RBCs.

2.6. Purification of P. vivax hemozoin

Packed RBC volumes from 460 to 650 μl from a mL of whole blood from each of the 3 monkeys infected with the three separate *P. vivax* isolates were split into 4 tubes of equal volume, for quadruplicate quantitation of hemozoin. Aliquoted packed RBCs were diluted 1:5 in DI H_2O and sonicated. The lysate was spun down at 14,000x g for 20 min. Resuspended pellets were washed twice in 1 ml of 2% SDS to solubilize membranes. Hemozoin pellets were washed twice in 1 ml DI H_2O before final pellet resuspension in 10 μl DI H_2O. No proteinase K treatment was conducted due to the limited amount of *P. vivax* sample and the absence of liver or spleen tissue to digest. Hemozoin was purified and quantitated using the above SDS bicarbonate/NaOH decrystallization method and the total amount of hemozoin produced per 10^{10} *P. vivax* parasites was calculated.

3. Results

3.1. Microscopy shows CR and CS P. berghei hemozoin production and host tissue accumulation

No brown pigment particles or birefringent crystals are seen in the blood of uninfected animals (Fig. 1A and B). Brightfield examination of Geimsa blood films shows CS *P. berghei* parasites infect normocytes and reticulocytes, often have multiple parasites per infected erythrocyte and produce dark intracellular pigment particles consistent with hemozoin (Fig. 1C). Overlapping polarized light micrographs demonstrate that the position of the brown pigment corresponds directly to areas of birefringence (Fig. 1D). Blood films from CR and CRCT *P. berghei* have much less birefringent crystals (Fig. 1E–H).

Histological examination of livers and spleens under brightfield and polarizing light microscopy demonstrates that CS as well as CR parasites produced hemozoin that heterogeneously accumulates in liver and spleen (Figs. 2 and 3, respectively). Relatively less birefringent, brown crystal accumulates in the liver and spleen of CR infected as compared to CS infected animals with the least accumulation being in CRCT animals (Figs. 2 and 3). No brown pigment or birefringent crystals are visualized in liver (Fig. 2A and B) or spleen (Fig. 3A and B) of uninfected animals.

Examination of hemozoin purified from blood samples by FEISEM demonstrated the occurrence of crystals consistent with hemozoin in the blood of CS infected mice (Fig. 4A). Hemozoin was not purified from the blood of CR or CRCT *P. berghei* infected mice in sufficient quantities to allow for characterization of blood hemozoin by FEISEM. However, crystals morphologically identical to wild type CS hemozoin were identified by FEISEM in combined liver and spleen tissue isolated from either CR or CRCT infected animals (Fig. 4B–D). CR *P. berghei* forms roughly 70 nm × 70 nm × 200 nm

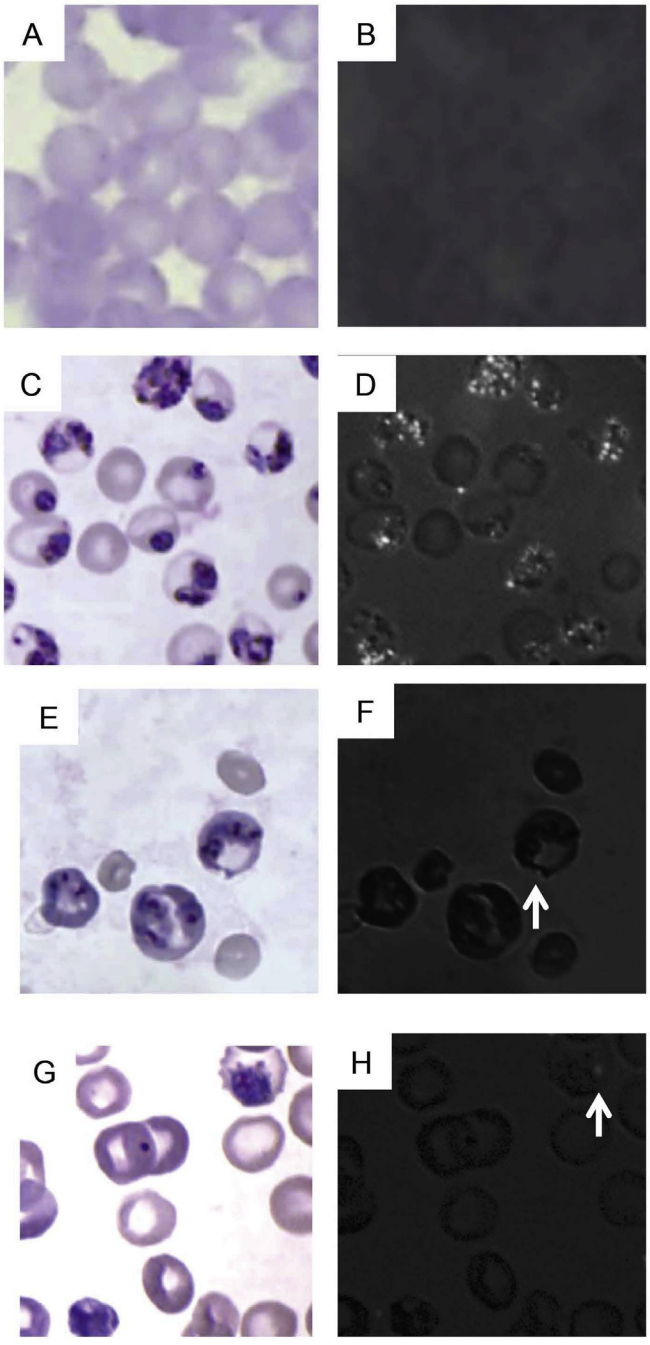

Fig. 1. Photomicrographs of Geimsa stained blood smears from: An uninfected mouse (1A, B), a CS infected mouse (1C, D), a CR infected (1E, F), and a CR infected chloroquine treated mouse (1G, H). Fig. 1B, D, F and H are photomicrographs of the same fields taken under polarizing light. Birefringent crystals appear as intracellular points of light. The arrows in F and H indicate a single visible hemozoin crystal. Total magnification = 1000x.

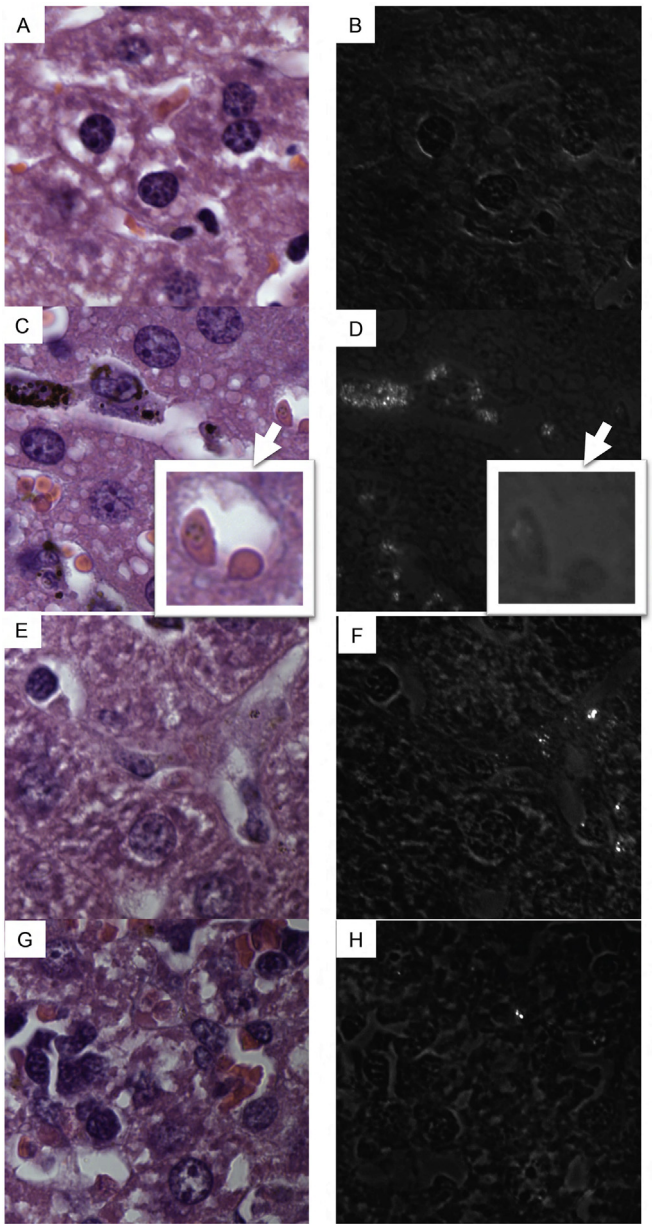

Fig. 2. Histological photomicrographs of H + E stained liver sections from: An uninfected mouse (2A, B), a CS infected mouse (2C, D), a CR infected mouse (2E, F), and a CR infected chloroquine treated mouse (2G, H). Fig. 2B, D, F and H are photomicrographs of these identical fields taken under polarizing light. Areas of extracelllar accumulation of birefringent crystal in liver appear as white areas. Inset in sections C and D show an infected erythrocyte on the left which polarizes light on darkfield. Total magnification = 1000x.

smooth faced crystals in the presence or absence of chloroquine. In contrast the CS *P. berghei* crystals were 135% larger along a single width or height face at 95 nm × 95 nm × 200 + nm. No crystals were observed in the uninfected group. CR strain *P. berghei* forms hemozoin crystals morphologically identical to hemozoin produced by wild type CS *P. berghei*.

3.2. Hemozoin production differs between strains

On the day of exsanguination, mean hematocrit values were roughly two-fold higher in the blood of uninfected animals; 43% (±2.4) as compared to CRCT mice at 23.5% (±6.8%), CS mice at 20% (±2.2%), and CR mice at 15.8% (±1.7%) (Table 1). Mean percent of infected erythrocytes at time of exsanguination ranged from a CS group high of 69% (total intraerythrocytic parasites/total RBCs) to 29% for the CR group and 15% for the CRCT group (Table 1). Mouse 1 in the CR/CT group was of interest in that its 4% parasitemia was substantially lower than the other 3 members of this group.

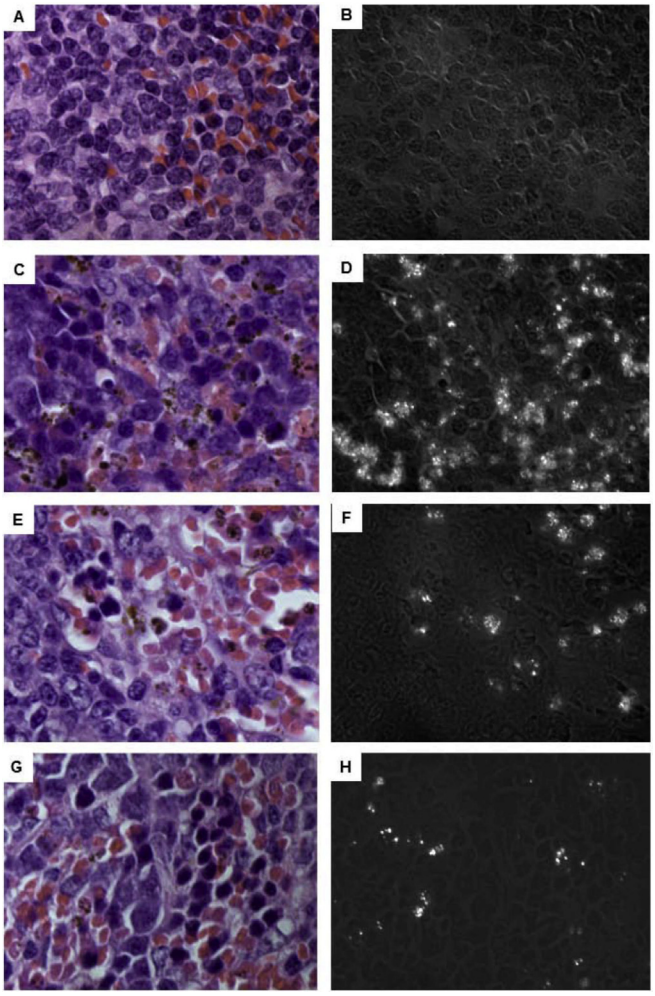

Fig. 3. Histological photomicrographs of H + E stained spleen sections from: An uninfected mouse (3A, B), a CS infected mouse (3C, D), a CR infected mouse (3E, F), and a CR infected chloroquine treated mouse (3G, H). Fig. 3B, D, F and H are photomicrographs of these identical fields taken under polarizing light. Areas of accumulation of birefringent crystal in spleen appear as white points. Total magnification = 1000x.

Because of multiple parasites invading a single erythrocyte we also counted the total number of parasites per 1000 erythrocytes to normalize total parasites. The means were 1303, 897 and 464 per 1000 erythrocytes respectively for CS, CR and CRCT *P. berghei*.

Spectrophotometric hemozoin quantitation (OD 400 nm) showed highest mean hemozoin content to be in the blood of CS strain infected mice followed by the CR group and CRCT groups respectively (Table 1). Thus in blood, CR and CRCT hemozoin was reduced 69-fold and 8640-fold, respectively, relative to the CS wild type with total parasite number at time of blood isolation reduced only by 1.5-fold and 2.8-fold using parasite number (parasitemia reduction is 2.3 and 4.6 fold using percent infected erythrocytes) in CR and CRCT *P. berghei*. We processed up to 320 μl of plasma per mouse for hemozoin, but in all groups the yield was 0 nmoles of hemozoin. Hemozoin in spleens ranged from a mean total of 160 (±25.1) nmoles per spleen for the CS infected mice to 29.7 (±13.3) nmoles for the CR group as determined by measurement at OD-400 (Table 1). Splenic hemozoin was therefore reduced only 5.4-fold in the CR group. Mean hemozoin was 6.6 nmoles in the spleen of CRCT group mice for a 24.2-fold reduction as compared to the CS group mean. Spleens and livers of CR and CRCT infected mice were slightly yet significantly larger than CS mice and spleens of CR, CRCT and CS mice were greatly enlarged as compared to uninfected mice (Table 1). For liver the average amount of hemozoin was: 2266.5 (±262.4) nmoles for CS, 736.2 (±218) nmoles for CR and 47.8 (±18.4) nmoles for CRCT. The amount of hemozoin in liver was thus 3.1-fold and 47.4-fold reduced in CR and CRCT groups, respectively, as compared to the average CS liver (Table 1). The highest accumulation of hemozoin was found in liver followed by spleen and blood in all cases with the exception of CS blood, which contained more hemozoin than CS spleen. This was likely a result of the shorter time post infection period and higher parasitemia at exsanguination for the CS infected group (Fig. 5).

The summed totals for nmoles of hemozoin detected in blood + spleen + liver were: 4155 (±333.2) for CS infected mice, 791 (±231.7) for CR infected mice and 53.8 (±26.7) for CRCT infected mice. Therefore, CR infect mice contained 5.4-fold less hemozoin than CS infected mice by the time of exsanguination. CRCT mice contain 76.1-fold less than the CS mice and 14.1-fold less hemozoin than CR mice. For CS *P. berghei* blood, spleen and liver were 42%, 4% and 54% of the total hemozoin. For CR *P. berghei* blood, spleen and liver were 3%, 4% and 93% of the total hemozoin. For CRCT *P. berghei* blood, spleen and liver were 0.3%, 12% and 87% of the total hemozoin.

3.3. LDMS-analysis identifies hemozoin specific heme signature

LDMS definitively identified the m/z heme signature consistent with hemozoin crystals in the blood, spleen and livers of CS, CR and CRCT infected mice. LDMS detected plasma hemozoin only in CS infected mice. LDMS did not detect hemozoin in the blood of uninfected animals (Fig. 5). Hemozoin was detected in the blood of ¼ CRCT mice, ¾ CR mice and all CS mice. Tissue hemozoin specific heme ion intensities were highest for CS infected mice followed by CR and CRCT mice respectively and were not detected in uninfected mice (Supplementary Fig. S1). CS liver heme ion intensities were approximately 10-fold higher than in CS spleens. This is in keeping with the general colorimetric assay observation that more hemozoin is found in liver than spleen. In spleen, CS and CR heme ion amplitudes were comparable, though detector plate saturation of the LDMS may have occurred. CR liver heme ion hemozoin intensity was 18.5-fold higher than in CRCT livers, and CR spleen intensities 12.8-fold higher than in CRCT spleens. Normalization of intergroup hemozoin heme ion amplitudes for uniform parasite number indicates that CR parasites produce 3.1-fold less hemozoin than do CS parasites while CRCT parasites produce 68.9-fold less hemozoin than do CS parasites. This is consistent with the 5-fold and 76-fold reduction in hemozoin production observed for CR and CRCT compared to CS via spectrophotometric analysis and is likewise consistent with observations made under brightfield and polarizing light microscopy and FEISEM.

3.4. Neutral lipids associated with P. berghei hemozoin

Hemozoin from both CS and CR *P. berghei* may exist in a similar lipid environment for formation. Sucrose cushion purification of hemozoin from both CS and CR *P. berghei* in blood copurifies detectable amounts of the monoacylglycerides monopalmitic glycerol (MPG) (337 m/z) and monostearic glycerol (MSG) (365 m/z) (Fig. 6A). These lipids are identified in wild type CS *P. berghei* intact parasites isolated by saponin (Fig. 6B) and to a lesser extent in sucrose gradient purified hemozoin from bloodstage CR *P. berghei* (Fig. 6C). The identity of MPG and MSG in sucrose purified hemozoin and CS *P. berghei* parasites was confirmed by MS/MS analysis as shown in Supplementary Fig. 2, 3 and 4.

In summary, MSG and MPG appear to be the dominant MAG

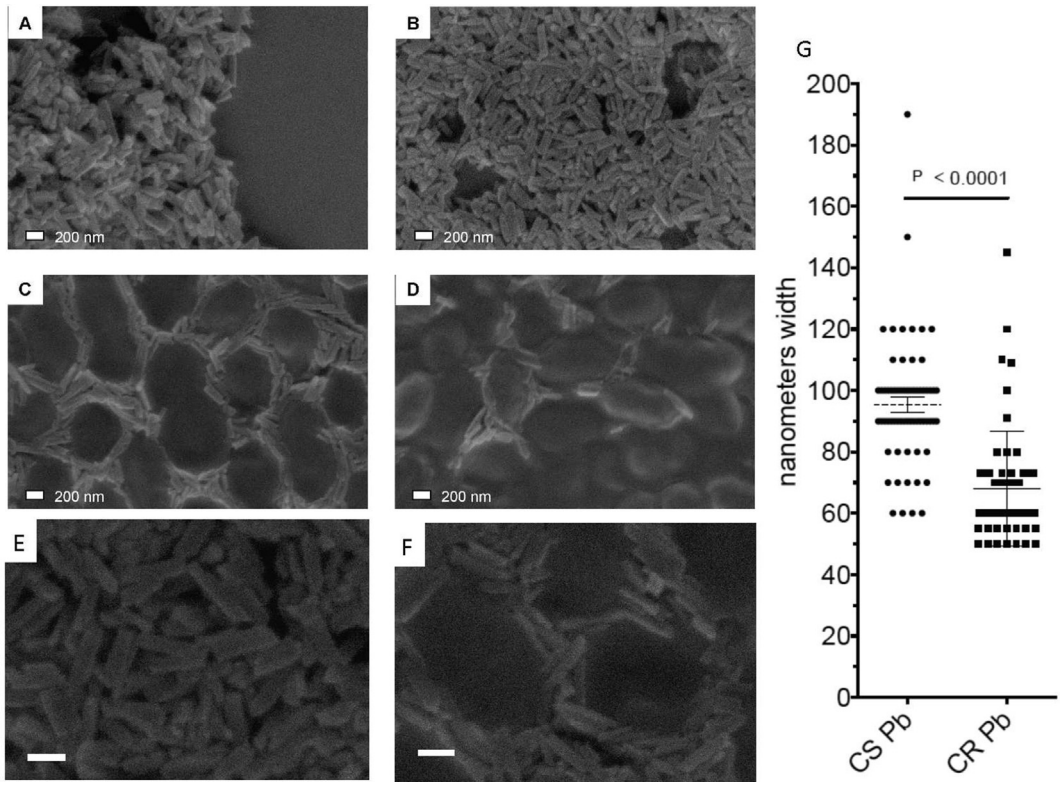

Fig. 4. Field emission in lens scanning electron micrographs of: hemozoin isolated from CS blood (4A), CS tissue (4B), CR tissue (4C) and CRCT tissue (4D). Total magnification = 74,000 x A-D; 100,000 x (4E and F). Measurement of crystal width has average width in CS P. berghei (CS Pb) as 95 nm (n = 64) and for CR P. berghei (CR Pb) as 70 nm (n = 54) with $p < 0.0001$ (4G).

Table 1
Spectrophotometric quantification of hemozoin in blood, spleens and livers.

		CS	CR	CRCT	Uninfected
Blood	% Hematocrit	20 ± 2.2	15.8 ± 1.7	23.5 ± 6.8	43 ± 2.4
	Percent infected erythrocytes	69%	29%	15%	0%
	Parasites per 1000 erythrocytes	1303 ± 214	897 ± 379	464 ± 298	0
	Volume blood processed μl	400	400	400	400
	nmoles hz./ml.	864.1 ± 191.5	12.7 ± 1.05	0.1 ± 0.03	0.03 ± 0.002
	nmoles hz. blood total	1728.2 ± 383	25.3 ± 2.1	0.2 ± 0.06	0.06 ± 0.004
Spleen	Weight (mg.)	233 ± 22	867 ± 84	928 ± 143	76 ± 9
	mg processed	186 ± 22	693 ± 84	742 ± 143	61 ± 9
	nmoles hz./gm.	682 ± 116	34 ± 20	10 ± 7	3.9 ± 1.1
	nmoles hz spleen total weight	160 ± 26	29.7 ± 13.8	6.6 ± 6.9	0.3 ± 0.1
Liver	Weight (mg.)	1482 ± 97	2104 ± 34	2276 ± 501	1559 ± 96
	mg processed	1142 ± 97	1683 ± 34	1821 ± 501	1247 ± 96
	nmoles hz./gm.	1530 ± 177	350 ± 100	21 ± 10	0.3 ± 0.02
	nmoles hz liver total weight	2266 ± 262	736 ± 217	47 ± 18	0.67 ± 0.028
Total	nmoles hz. average mouse	4155 ± 333	790 ± 231	54 ± 26	NA

Blood, spleen and liver hemozoin was isolated, decrystallized by NaOH treatment and quantified via OD 400 nm. CS *P. berghei* infected mice had highest hemozoin (hz.) accumulations followed by CR and CR/CT infected mice. CR parasites produce 0.49 μmoles of hemozoin per 10^{10}, or one fourth as much as an equivalent number of CS parasites. Chloroquine treatment attenuates production of hemozoin by CR parasites roughly 16-fold as compared to chloroquine untreated CR *P. berghei*.

neutral lipids associated with sucrose purified hemozoin in *P. berghei* while little to no saturated MOG or MLG is seen. As with CS *P. berghei*, sucrose purified hemozoin from CR *P. berghei* also contains above background MPG and MSG as verified by MS2 analysis (Supplementary Fig. 4A and D) and absent MLG and MOG (Supplementary Fig. 3, 4B and 4C).

3.5. Quantitation of *P. vivax* hemozoin production by strain

In *P. vivax* both CS and CR isolates inhabit reticulocytes similar to CR *P. berghei*. The CS Sal 1 parasitemia was 8200/μl while CR Indo Strain was 6900/μl. Hemoglobin content was slightly lower in the Indo strain. After normalization for parasitemia and host cells as determined by hemoglobin content, colorimetric measurements of decrystallized hemozoin isolated from a mL of whole blood indicated that 3.29 ± 1.1 and 4.55 ± 0.8 μmol of hemozoin are produced

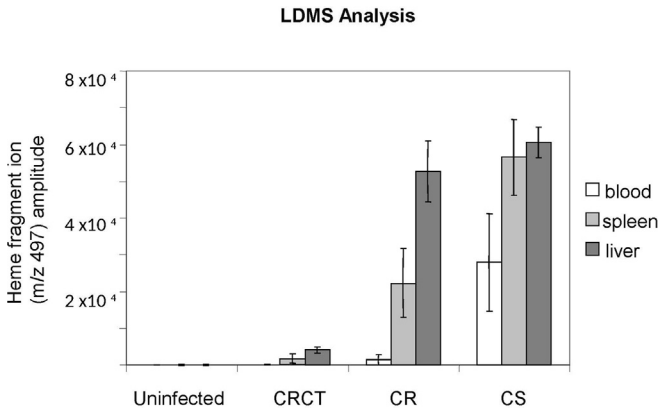

Fig. 5. Blood and tissue samples from uninfected, CS, CR and CR/CT infected mice were diluted 1:5 in PBS and assayed by LD/MS using the Applied Biosystems Voyager DE-STR instrument. For each mouse (4 mice per group) 5 LDMS measurements were conducted. Each measurement consisted of twenty laser shot spectra. These 20 shot spectra were averaged and the averaged mVolt heme specific amplitudes were graphed. LDMS indicates that quantitatively more hemozoin was present in CS infected mice as compared to CR infected mice. There was a further dramatic reduction in the amount of hemozoin detected by LDMS in CR/CT mice as compared to CR drug untreated mice. In all groups the highest hemozoin levels were identified in liver followed by spleen with the lowest amount of hemozoin being present in blood.

per 10^{10} Indo and Sal-I, respectively. That is to say only 1.4 fold more hemozoin was produced by the CS *P. vivax* strain than the CR *P. vivax* strain, which is within error in measurement. Giemsa and polarized microscopy show similar hemozoin in CS and CR *P. vivax* (Fig. 7).

4. Discussion

The worldwide distribution and incidence of CR *P. vivax* has expanded significantly since emerging in Papua New Guinea in 1989 (Rieckmann et al., 1989) (Goncalves et al., 2014). Understanding into the molecular basis of alternative forms of chloroquine resistance is needed to retain quinolines as effective frontline drugs (Baird et al., 2012). In this study, hemozoin production and distribution was analyzed in blood, spleen and liver tissue from CR or CS *P. berghei* infected mice. Results found that 1830 (±210) nmoles hemozoin are produced per 10^{10} asynchronous NYU-2 CS strain *P. berghei* parasites in blood circulation. This is consistent with the CS strain's hemozoin levels previously measured by Fitch of 2100 (±360) nmoles per ml of packed male Swiss mouse iRBCs. For CR *P. berghei* infected mice, the hematocrit adjusted quantitation of 80.14 (±13.48) nmoles per 10^{10} is consistent with the previously reported 71 ± 16 for the CR strain (Fitch and Chou, 1997). Therefore, circulating CR *P. berghei* parasites contain only 3–4% of the hemozoin content of CS strain infected blood cells. Blood film microscopic analysis is generally supportive of the long held designation of the CR strain as lacking substantial hemozoin and thus being unpigmented. However, evaluation of tissue hemozoin in liver and spleen of CR infected mice clearly shows that measurement of blood hemozoin alone is an inaccurate indication of actual hemozoin production by CR strain *P. berghei*. This agrees with older data of a ring predominance in the blood with CR *P. berghei* with substantial measurable schizonts in the spleen (Schneider, 1968) and liver (Jacobs and Warren, 1967). In previous studies 95% of residual hemozoin persistent for months is present in the liver and spleen of murine malaria (Levesque, 1999). On a normalized per parasite basis at the time of exsanguination CR *P. berghei* achieves close to a 28% total hemozoin production capacity compared with the CS strain, and the CRCT *P. berghei* is 4% of

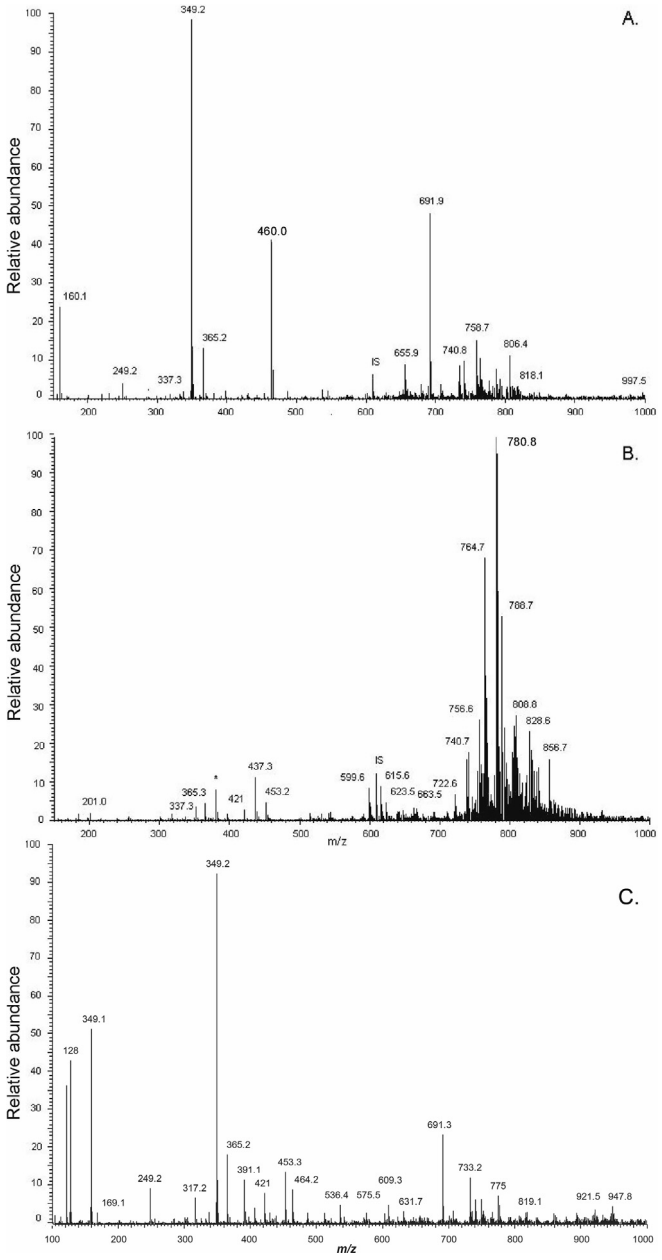

Fig. 6. ESI-MS analysis of sucrose purified hemozoin from CS *P. berghei* parasites indicates copurification of the saturated monoacylglycerides MPG (337 m/z) and MSG (365 m/z) (6A). These lipids are also observed in intact CS *P. berghei* parasites, which demonstrate abundant phospholipids in the 750–850 m/z range (6B). CR *P. berghei* also has above background MPG and MSG (6C). Prior analysis indicates the major peak at 349 m/z is residual sucrose.

CS *P. berghei* ([CR total hemozoinxCS parasite #]/[CS total hemozoinxCR parasite #]).

Chloroquine treatment significantly inhibits hemozoin production by CR *P. berghei* while allowing multiplication of viable parasites to about 15% parasitemia. Chloroquine treatment reduced total hemozoin production by 99% compared to CS and 93% compared to CR off chloroquine. This contrasts CR *P. falciparum* where a low to moderate dose of 100 nm/ml chloroquine leads to an increase in hemozoin production (Orjih et al., 1994). This finding highlights the disparate nature of species-level chloroquine resistance phenotypes present in the genus *Plasmodium* (Orjuela-

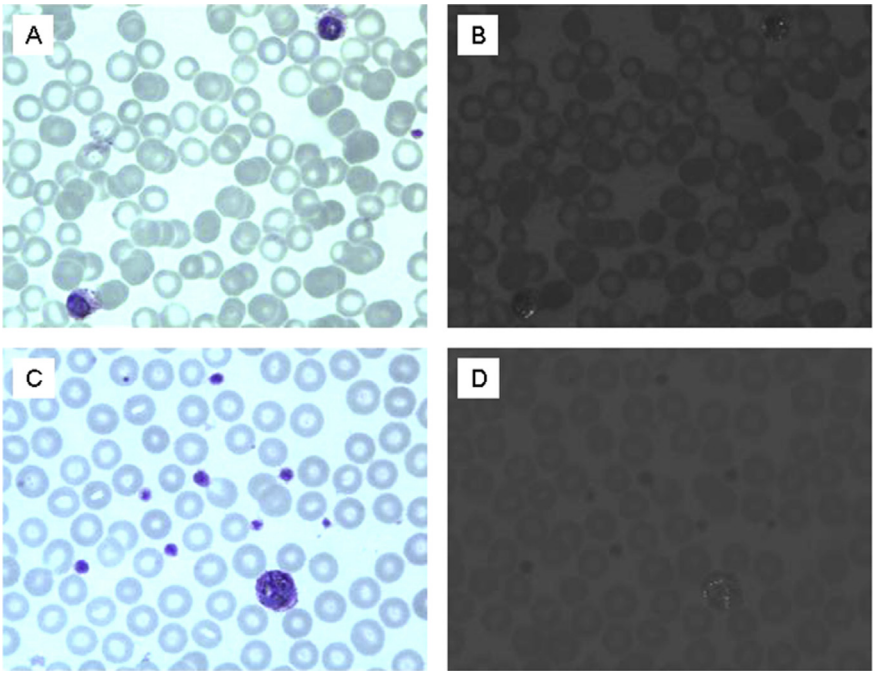

Fig. 7. Photomicrographs of Geimsa stained blood smears from: CS *P. vivax* Sal 1 (7A), CR *P. vivax* Ind (7C), and photomicrographs of the same fields taken under polarizing light: CS *P. vivax* Sal 1 (7B), CR *P. vivax* Ind (7D). Total magnification = 1000x.

Sanchez et al., 2009). In *P. falciparum* from 4 to 10 μmoles of hemozoin is reportedly formed per 10^{10} late trophozoite stage parasites (Orjih and Fitch, 1993; Zhang et al., 1999). Gligorijevic reports up to 15 μmoles produced by the late trophozoite to early schizont transition in *P. falciparum* with little productivity difference seen between CR and CS strains (Gligorijevic et al., 2006). This is supported by Zhang and Ginsburg while a somewhat older measurement of 9.60 μmoles per 10^{10} CS versus 5.15 for CR has also been reported (Orjih and Fitch, 1993).

Roughly 50% higher chloroquine dosage is required to impart an equivalent level of inhibition than when CS *P. berghei* grows in the reticulocyte (Dei-Cas et al., 1984). Clearly, CR strain specific factors in conjunction with reticulocyte specific host cell conditions contribute to resistance. An important morphological difference between sensitive and resistant *P. berghei* is the digestive vacuole. In CS parasites abundant intracellular hemozoin crystals are seen in a single digestive vacuole while 2 or 3 smaller vacuoles generally devoid of pigment are usually present in CR strains (Saxena et al., 1989). Ultrastructural studies indicate disruption of the normal cytosomal tube system in drug resistant parasites with only small, double membrane cytoplasmic food vesicles derived by micropinocytosis; only in infected mature erythrocytes does both micropinocytosis and cytosomal ingestion occur (Slomianny et al., 1985; Slomianny, 1990; Slomianny and Prensier, 1990). Paradoxically, the rate of hemoglobin catabolism appears higher in *P. berghei* infected reticulocytes than mature erythrocytes despite the lack of a cytosomal system. This counters the notion that the reported lack of free heme and pigment in CR *P. berghei* can be explained by a failure of the CR strain to digest hemoglobin resulting from access to some alternative reticulocyte-specific nutrient source. While hemoglobin catabolism rates are comparable in rat reticulocytes infected with either CS or CR *P. berghei*, CR infected reticulocytes contained less total heme which is apparently coupled to a net loss of heme from the CR infected cell (Wood and Eaton, 1993). This is in agreement with the observation that free heme is absent from CR and CRCT parasites (Fitch and Chou, 1997).

Slomianny originally proposed that hemozoin is generally not seen accumulated intracellularly in CR *P. berghei* because it is expelled from the developing reticulocyte via exosomal release (Slomianny et al, 1985). As demonstrated by LDMS, optical spectrometry, tissue histology and FEISEM, significant accumulation of hemozoin in liver and spleens of CR *P. berghei* infected mice but not the uninfected mice is consistent with CR *P. berghei* producing significant hemozoin. We noted the hemozoin was 70% smaller in width of a single face in the CR *P. berghei*. A major limitation of our study is not being able to measure hemozoin production with equal numbers of CR and CS *P. berghei* grown *ex vivo* in culture, which would provide a side by side cellular comparison in addition to the organ quantification reported here.

Bannister and coworkers also published microscopic evidence of exosomal export vesicles in *P. falciparum* (Bannister et al., 2004). Exosomes from *Plasmodium yoelii* infected reticulocytes contain parasite derived components suggesting *Plasmodium* species can access the host cell's export process (Martin-Jaular et al., 2011). Subversion of the native exocytosis pathway might provide parasites with a resistance mechanism whereby chloroquine, known to bind heme and hemozoin, can be expelled from the cell along with pigment. Exocytosis is a known drug resistance mechanism in other types of eukaryotic cells (Azmi et al., 2013). Alternatively, there could be sequestration of late trophozoites and schizonts in the tissues, which mask blood stage hemozoin. We do see trophozoites from bloodstage CR and CRCT parasites and isolated hemozoin from these mice is detectable by mass spectrometry, and biochemical means with a small amount seen in blood films.

Hemozoin-associated monoacylglycerides such as MPG have been implicated as catalyzing heme crystal formation (Egan et al., 2006) (Ambele et al., 2013). Here, saturated monoacylglycerides observed in close association with sucrose purified hemozoin isolated from blood stage parasites, namely MPG and MSG, were conserved in CS and CR *P. berghei* (Fig. 6). That these neutral lipids

are consistently associated with hemozoin and occur at relatively stable ratios in both *P. falciparum* and *P. berghei* suggests a conserved mechanism for hemozoin formation may exist (Pisciotta et al., 2007). Neutral lipid compositional differences probably do not primarily mediate chloroquine resistance (Supplementary Fig 2-4). This is consistent with this the morphological uniformity in the crystal structure seen between hemozoin purified from the CS, CR and CRCT infected mice (Fig. 4). Insufficient material was available to determine if neutral lipids are associated with *P. vivax* hemozoin.

Literature comparing hemozoin production in CR and CS strains of *P. vivax* of is lacking. Here, we observed CR *P. vivax* produced 72% of the hemozoin compared to CS *P. vivax*, although the monkey sample size was low. This suggests the mechanism of chloroquine resistance in *P. vivax* may differ from *P. berghei*. Considering the asynchronous nature of *P. vivax*, the hemozoin yields of 3–4 μmoles per 10^{10} parasites suggest *P. vivax* produces hemozoin at close to the same rate as *P. falciparum*.

Acknowledgements

We thank Coy D. Fitch (deceased) for experimental design input and for performance of the mouse studies. Joanne Sullivan and John Barnwell at the CDC generously provided the chloroquine resistant and drug sensitive *P. vivax* samples. We thank Lirong Shi for technical support. The AB-Mass Spectrometry Facility at the Johns Hopkins School of Medicine is funded by National Center for Research Resources Shared-Instrument Grant 1S10-RR14702. This work was supported by grants from Pew Scholars Program in Biomedical Sciences 2000 (DJS) and NIH RO1 AI45774-01. A NCCR Grant GPDGCRC RR0052 supports the use of RBC for culturing *P. falciparum* for hemozoin.

Appendix A. Supplementary data

Supplementary data related to this article can be found at http://dx.doi.org/10.1016/j.ijpddr.2017.02.001.

References

Ambele, M.A., Sewell, B.T., Cummings, F.R., Smith, P.J., Egan, T.J., 2013. Synthetic hemozoin (beta-Hematin) crystals nucleate at the surface of neutral lipid droplets that control their sizes. Cryst. Growth Des. 13.

Azmi, A.S., Bao, B., Sarkar, F.H., 2013. Exosomes in cancer development, metastasis, and drug resistance: a comprehensive review. Cancer Metastasis Rev. 32, 623–642.

Baird, K.J., Maguire, J.D., Price, R.N., 2012. Diagnosis and treatment of *Plasmodium vivax* malaria. Adv. Parasitol. 80, 203–270.

Bannister, L.H., Hopkins, J.M., Margos, G., Dluzewski, A.R., Mitchell, G.H., 2004. Three-dimensional ultrastructure of the ring stage of *Plasmodium falciparum*: evidence for export pathways. Microsc. Microanal. 10, 551–562.

Das, S., Chakraborty, S.P., Hati, A.K., Roy, S., 2013. Association between prevalence of chloroquine resistance and unusual mutation in pfmdr-I and pfcrt genes in India. Am. J. Trop. Med. Hyg. 88, 828–834.

Dei-Cas, E., Slomianny, C., Prensier, G., Vernes, A., Colin, J.J., Verhaeghe, A., Savage, A., Charet, P., 1984. Preferential action of chloroquine on *Plasmodium* within mature erythrocytes. Pathol. Biol. Paris. 32, 1019–1023.

Egan, T.J., Chen, J.Y., de Villiers, K.A., Mabotha, T.E., Naidoo, K.J., Ncokazi, K.K., Langford, S.J., McNaughton, D., Pandiancherri, S., Wood, B.R., 2006. Haemozoin (beta-haematin) biomineralization occurs by self-assembly near the lipid/water interface. FEBS Lett. 580, 5105–5110.

Espinosa, D.A., Yadava, A., Angov, E., Maurizio, P.L., Ockenhouse, C.F., Zavala, F., 2013. Development of a chimeric *Plasmodium berghei* strain expressing the repeat region of the *P. vivax* circumsporozoite protein for in vivo evaluation of vaccine efficacy. Infect. Immun. 81, 2882–2887.

Fidock, D.A., Nomura, T., Talley, A.K., Cooper, R.A., Dzekunov, S.M., Ferdig, M.T., Ursos, L.M., Sidhu, A.B., Naude, B., Deitsch, K.W., Su, X.Z., Wootton, J.C., Roepe, P.D., Wellems, T.E., 2000. Mutations in the *P. falciparum* digestive vacuole transmembrane protein PfCRT and evidence for their role in chloroquine resistance. Mol. Cell 6, 861–871.

Fitch, C.D., Yunis, N.G., Chevli, R., Gonzalez, Y., 1974. High-affinity accumulation of chloroquine by mouse erythrocytes infected with *Plasmodium berghei*. J. Clin. Invest. 54 (1), 24–33.

Fitch, C.D., Chou, A.C., 1997. Regulation of heme polymerizing activity and the antimalarial action of chloroquine. Antimicrob. Agents Chemother. 41, 2461.

Foote, S.J., Kemp, D.J., 1989. Chromosomes of malaria parasites. Trends Genet. 5, 337–342.

Ginsburg, H., Famin, O., Zhang, J., Krugliak, M., 1998. Inhibition of glutathione-dependent degradation of heme by chloroquine and amodiaquine as a possible basis for their antimalarial mode of action. Biochem. Pharmacol. 56, 1305–1313.

Gligorijevic, B., McAllister, R., Urbach, J.S., Roepe, P.D., 2006. Spinning disk confocal microscopy of live, intraerythrocytic malarial parasites. 1. Quantification of hemozoin development for drug sensitive versus resistant malaria. Biochemistry 45, 12400–12410.

Goncalves, L.A., Cravo, P., Ferreira, M.U., 2014. Emerging *Plasmodium vivax* resistance to chloroquine in South America: an overview. Mem. Inst. Oswaldo Cruz 109, 534–539.

Ham, B.M., Jacob, J.T., Keese, M.M., Cole, R.B., 2004. Identification, quantification and comparison of major non-polar lipids in normal and dry eye tear lipidomes by electrospray tandem mass spectrometry. J. Mass Spectrom. 39, 1321–1336.

Howard, E.M., Zhang, H., Roepe, P.D., 2002. A novel transporter, Pfcrt, confers antimalarial drug resistance. J. Membr. Biol. 190, 1–8.

Jacobs, R., Warren, M., 1967. Sequestration of schizonts in the deep tissues of mice infected with chloroquine-resistant *Plasmodium berghei*. Trans. R. Soc. Trop. Med. Hyg. 61 (2), 273–275.

Levesque, M.A., Sullivan, A.D., Meshnick, S.R., 1999. Splenic and hepatic hemozoin in mice after malaria parasite clearance. J. Parasitol. 85 (3), 570–573.

Lin, J.W., Spaccapelo, R., Schwarzer, E., Sajid, M., Annoura, T., Deroost, K., Ravelli, R.B., Aime, E., Capuccini, B., Mommaas-Kienhuis, A.M., O'Toole, T., Prins, F., Franke-Fayard, B.M., Ramesar, J., Chevalley-Maurel, S., Kroeze, H., Koster, A.J., Tanke, H.J., Crisanti, A., Langhorne, J., Arese, P., Van den Steen, P.E., Janse, C.J., Khan, S.M., 2015. Replication of *Plasmodium* in reticulocytes can occur without hemozoin formation, resulting in chloroquine resistance. J. Exp. Med. 212, 893–903.

Martin-Jaular, L., Nakayasu, E.S., Ferrer, M., Almeida, I.C., Del Portillo, H.A., 2011. Exosomes from *Plasmodium yoelii*-infected reticulocytes protect mice from lethal infections. PLoS One 6, e26588.

Melo, G.C., Monteiro, W.M., Siqueira, A.M., Silva, S.R., Magalhaes, B.M., Alencar, A.C., Kuehn, A., del Portillo, H.A., Fernandez-Becerra, C., Lacerda, M.V., 2014. Expression levels of pvcrt-o and pvmdr-1 are associated with chloroquine resistance and severe *Plasmodium vivax* malaria in patients of the Brazilian Amazon. PLoS One 9, e105922.

Ocampo, M., Vera, R., Eduardo Rodriguez, L., Curtidor, H., Urquiza, M., Suarez, J., Garcia, J., Puentes, A., Lopez, R., Trujillo, M., 2002. *Plasmodium vivax* Duffy binding protein peptides specifically bind to reticulocytes. Peptides 23, 13–22.

Orjih, A., Ryerse, J., Fitch, C., 1994. Hemoglobin catabolism and the killing of intraerythrocytic *Plasmodium falciparum* by chloroquine. Cell. Mol. Life Sci. 50, 34–39.

Orjih, A.U., Fitch, C.D., 1993. Hemozoin production by *Plasmodium falciparum*: variation with strain and exposure to chloroquine. Biochim. Biophys. Acta 1157, 270–274.

Orjuela-Sanchez, P., de Santana Filho, F.S., Machado-Lima, A., Chehuan, Y.F., Costa, M.R., Alecrim, M.G., del Portillo, H.A., 2009. Analysis of single-nucleotide polymorphisms in the crt-o and mdr1 genes of *Plasmodium vivax* among chloroquine-resistant isolates from the Brazilian Amazon region. Antimicrob. Agents Chemother. 53, 3561–3564.

Peters, W., 1964. Pigment Formation and Nuclear Division in Chloroquine-resistant Malaria Parasites (*Plasmodium Berghei*, Vincke and Lips, 1948).

Peters, W., Ekong, R., Robinson, B., Warhurst, D., Pan, X.Q., 1990. The chemotherapy of rodent malaria. XLV. Reversal of chloroquine resistance in rodent and human *Plasmodium* by antihistaminic agents. Ann. Trop. Med. Parasitol. 84, 541.

Pisciotta, J.M., Coppens, I., Tripathi, A.K., Scholl, P.F., Shuman, J., Bajad, S., Shulaev, V., Sullivan Jr., D.J., 2007. The role of neutral lipid nanospheres in *Plasmodium falciparum* haem crystallization. Biochem. J. 402, 197–204.

Platel, D., Mangou, F., Tribouley-Duret, J., 1998. High-level chloroquine resistance of *Plasmodium berghei* is associated with multiple drug resistance and loss of reversal by calcium antagonists. Int. J. Parasitol. 28, 641–651.

Rieckmann, K.H., Davis, D.R., Hutton, D.C., 1989. *Plasmodium vivax* resistance to chloroquine? Lancet 2, 1183–1184.

Sá, J.M., Nomura, T., Neves, J.A., Baird, J.K., Wellems, T.E., del Portillo, H.A., 2005. *Plasmodium vivax*: allele variants of the mdr1 gene do not associate with chloroquine resistance among isolates from Brazil, Papua, and monkey-adapted strains. Exp. Parasitol. 109, 256–259.

Saxena, R., Kazim, M., Maitra, S.C., Dutta, G.P., 1989. Ultrastructural comparison of erythrocytic stages of experimentally selected drug resistant strains of rodent malaria parasite *P. berghei* with its susceptible strain. Indian J. Malariol. 26, 199–207.

Schneider, M.D., 1968. Characteristics and cross-resistance patterns of chloroquine-resistant *Plasmodium berghei* infections in mice, 1968 Aug Exp. Parasitol. 23 (1), 22–50.

Slomianny, C., 1990. Three-dimensional reconstruction of the feeding process of the malaria parasite. Blood Cells 16, 369–378.

Slomianny, C., Prensier, G., 1990. A cytochemical ultrastructural study of the lysosomal system of different species of malaria parasites. J. Protozool. 37, 465–470.

Slomianny, C., Prensier, G., Charet, P., 1985. Comparative ultrastructural study of the process of hemoglobin degradation by *P. berghei* (Vincke and Lips, 1948) as a

function of the state of maturity of the host cell. J. Protozool. 32, 1–5.
Sullivan, D.J., Gluzman, I.Y., Russell, D.G., Goldberg, D.E., 1996. On the molecular mechanism of chloroquine's antimalarial action. Proc. Natl. Acad. Sci. 93, 11865.
Vargas-Rodriguez Rdel, C., da Silva Bastos, M., Menezes, M.J., Orjuela-Sanchez, P., Ferreira, M.U., 2012. Single-nucleotide polymorphism and copy number variation of the multidrug resistance-1 locus of *Plasmodium vivax*: local and global patterns. Am. J. Trop. Med. Hyg. 87, 813–821.
Vega-Rodriguez, J., Pastrana-Mena, R., Crespo-Llado, K.N., Ortiz, J.G., Ferrer-Rodriguez, I., Serrano, A.E., 2015. Implications of glutathione levels in the *Plasmodium berghei* response to chloroquine and artemisinin. PLoS One 10, e0128212.
Wang, Q., Wang, M., Chang, H., Yang, B., 1998. Accumulation and effluxion of chloroquine in chloroquine-sensitive and chloroquine-resistant *Plasmodium berghei*. Zhongguo ji sheng chong xue yu ji sheng chong bing za zhi= Chin. J. Parasitol. Parasit. Dis. 16, 189.
Wellems, T.E., Plowe, C.V., 2001. Chloroquine-resistant malaria. J. Infect. Dis. 184, 770–776.
Wood, P.A., Eaton, J.W., 1993. Hemoglobin catabolism and host-parasite heme balance in chloroquine-sensitive and chloroquine-resistant *Plasmodium berghei* infections. Am. J. Trop. Med. Hyg. 48, 465–472.
Yayon, A., Bauminger, E., Ofer, S., Ginsburg, H., 1984. The malarial pigment in rat infected erythrocytes and its interaction with chloroquine. A Mössbauer effect study. J. Biol. Chem. 259, 8163–8167.
Zhang, J., Krugliak, M., Ginsburg, H., 1999. The fate of ferriprotorphyrin IX in malaria infected erythrocytes in conjunction with the mode of action of antimalarial drugs. Mol. Biochem. Parasitol. 99, 129–141.